

Reconstruction-induced multiple gaps in the weak coupling limit : the surface band of Au(111) vicinal surfaces

C. Didiot, Y. Fagot-Revurat, S. Pons, B. Kierren, C. Chatelain and D. Malterre[*]

Laboratoire de Physique des Matériaux UMR 7556, Université Henri Poincaré,

Nancy I - B.P. 239 F-54506 Vandœuvre-lès-Nancy, France

(Dated: February 24, 2006)

Opening of several gaps in the surface band structure of vicinal Au(23 23 21) surface has been evidenced by high resolution photoemission spectroscopy whereas the energy dependence of the surface electronic density have been determined by scanning tunneling spectroscopy. From a methodological point of view, the values of the gaps and the phase of the electronic density allow to estimate the reconstruction potential which yields the electronic Bragg diffraction, the gap formation and the modulation of the electronic density. These spectroscopic behaviors give a pedagogical illustration of one of the basic concepts of solid state physics.

PACS numbers: 73.20.At, 79.60.Bm, 68.37.Ef, 72.10.Fk

Translational symmetry leads to the concept of Bloch waves and their Bragg diffraction by the periodic potential results in electronic gaps. Similarly, in systems exhibiting a superperiodic surface structure, surface electrons experience the superperiodic potential yielding in principle band folding and gaps in the surface Brillouin zone. This was demonstrated in superlattice systems where the superperiodic potential is quite large, like periodic adsorbate films [1–4] and step arrays [5]. For example, photoemission measurements have evidenced the band folding in the periodic step edge potential of Shockley state in vicinal surfaces of noble metals. The step edge potential can even be sufficiently high to induce a one dimensional confinement of the surface state in terraces [6, 7]. But in systems where the superpotential is very weak like in the herringbone reconstruction of Au(111), its effect on the photoemission spectral function is quite undetectable [8]. The spectroscopic signature in photoemission are obscured by the existence of three different domains. However, due to its local character, Scanning Tunneling Spectroscopy (STS) has shown to be sensitive to the reconstruction of Au(111) surface [9, 10]. Differential conductance (dI/dV , which in a simple approach, is proportional to local density of states (LDOS)) images at different bias voltages have evidenced the localization of surface electronic density. Vicinal surfaces prevent the formation of domains and could allow the observation of superperiodic state in Angle-Resolved Photoemission Spectroscopy (ARPES). Recent measurements on different Au(111) vicinal surfaces nicely demonstrated the effect of steps on confinement but failed to show the superperiodicity associated with the reconstruction [11].

Here we report a high resolution ARPES and STS study of the surface electronic state in Au(23 23 21). Since the Shockley state in the direction perpendicular to the steps is confined in step edge-induced quantum well [11], we focus on the spectroscopic behavior in the parallel direction. By using the complementarity of the

two spectroscopies, we unambiguously show the effects of the weak reconstruction potential in the momentum and direct spaces. Firstly, ARPES evidences the Bragg diffraction of Shockley state associated with the reconstruction superperiodicity and allows the direct measurement of several gaps whose amplitudes reflect the Fourier components of the reconstruction potential. Secondly, STS can visualize the localization of the electronic wave function and its out-of-phase behavior through the gaps. The gap amplitudes and the electronic density phase allow us to determine the related Fourier components of the reconstruction.

The measurements were carried out in a UHV setup composed of a molecular beam epitaxy chamber for the elaboration and characterization of the surfaces, a Scanning Tunneling Microscopy (STM) chamber equipped with a 5K-Omicron STM and a photoemission chamber with a high resolution Scienta SES 200 analyser. The photoemission experiments were carried out at liquid nitrogen temperature with an angle resolution better than 0.3° (corresponding to a momentum resolution better than 0.010 \AA^{-1}) and an energy resolution better than 5 meV. The dI/dV maps were recorded at 5 K in the open feedback loop mode using the lock-in technique with a bias modulation of 10 meV at 700 Hz. The sample was cleaned by several cycles of Ar^+ etching and annealing at 500°C and it was characterized by STM and Auger Electron Spectroscopy (AES). In Figure 1(b), we present a STM image showing the topography of the Au(23 23 21) vicinal surface. This reconstruction, reminiscent to the herringbone one of flat Au(111), results from a uniaxial compression of the topmost atomic layer along the $(1\bar{1}0)$ direction [12]. In contrast to Au(111) reconstruction, the ridges are not parallel and are nearly perpendicular to steps as previously reported [13]. Moreover, the superperiodic cell ($L_{sp} = 66 \text{ \AA}$) is slightly larger than in Au(111) (63 \AA). As previously shown in the literature [11], the Shockley state in such a vicinal surface is very anisotropic : due to the step edge potential, it is

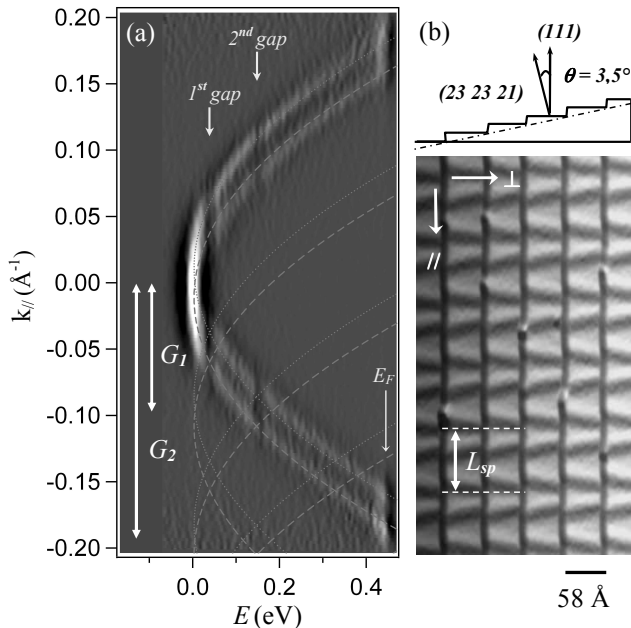


FIG. 1: (a) Second derivative of the ARPES intensity showing the spin-orbit splitting and the opening of two gaps centered at $E = 45$ meV and $E = 145$ meV. The dotted lines represents parabolas centered in the different Brillouin zones. (b) STM image evidencing the reconstruction lines on the terraces ($V_s = -0.7$ V, $I = 0.6$ nA).

confined in the direction perpendicular to the steps and exhibits a propagative character in the parallel direction with a nearly free electron dispersion. However, we were able to evidence reconstruction effects in the dispersion along the parallel direction. Fig.1(a) exhibits an intensity map representing the second energy derivative as a function of energy and wave vector. These ARPES data are dominated by two dispersive bands. They result from the well known spin-orbit interaction on Au Shockley state [14, 15]. The dispersion curves also exhibit low intensity stripes at $E_1 = 45$ meV and $E_2 = 145$ meV (the origin of energy has been chosen at the bottom of the surface band). These low intensity regions reflect the opening of reconstruction-induced gaps due to the superperiodic potential. Surprisingly for a nearly free electron system, the gap opening due to Bragg electronic diffraction does not occurs at the Brillouin zone boundary. This is due to the spin-orbit interaction which results in two k-shifted spin polarized Shockley bands. As Bragg diffraction does not affect the spin direction, it is encountered when bands with same spin are related by a reciprocal vector. Thus, it occurs at $k_{\pm} = \pi/L_{sp} \pm \Delta k_{s.o.}/2 = 0.0485 \pm 0.0115 \text{ \AA}^{-1}$ for the two spin-orbit bands as shown in Fig. 1(a) by the crossing of parabola centered in the second Brillouin zone. One can also check on Fig. 1(a) that the second gap also obeys the Bragg condition since it corresponds to the intersection with the parabola centered at

$4\pi/L_{sp} \pm \Delta k_{s.o.}/2$ and that there is no direct evidence of a gap corresponding to the third reciprocal vector. We would like to point out that there is no sizeable intensity in the folded bands and that the spectral weight is mainly localized along the parabola centered at $\bar{\Gamma}$. This behavior likely reflects the weakness of the reconstruction potential as recently suggested [16, 17] and explains why the reconstruction effect has not been observed before. A high energy and momentum resolution is needed to evidence these gap openings.

In figure 2(a), we report energy distribution curves (EDC) for several momenta through the first energy gap. For momenta smaller than the first gap k value ($k_+ = 0.037 \text{ \AA}^{-1}$), one nearly dispersionless feature at $E = 10$ meV can be observed in the EDC. With increasing k, this structure vanishes whereas two additional features successively appear at $E \simeq 55$ meV and shift with different dispersions to high energy. This spectral behavior

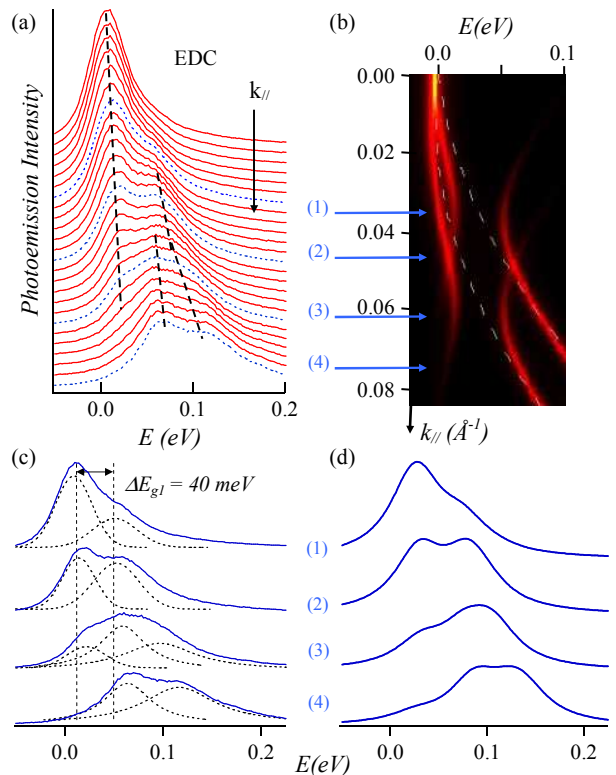


FIG. 2: (color online)(a) EDC spectra in the momentum range associated with the first gap. The blue dotted curves and blue arrows in (b) correspond to selected k values : 0.035 \AA^{-1} for (1), 0.048 \AA^{-1} for (2), 0.062 \AA^{-1} for (3) and 0.075 \AA^{-1} for (4) (dotted lines are guides for the eye). (b) Image representing the dispersion of the two spin orbit bands calculated in nearly free electron model (dotted lines represent the free electron dispersions). (c) Experimental EDC spectra for the selected k values. (d) Corresponding simulated spectra obtained by taking into account the lifetime and angular resolution broadenings.

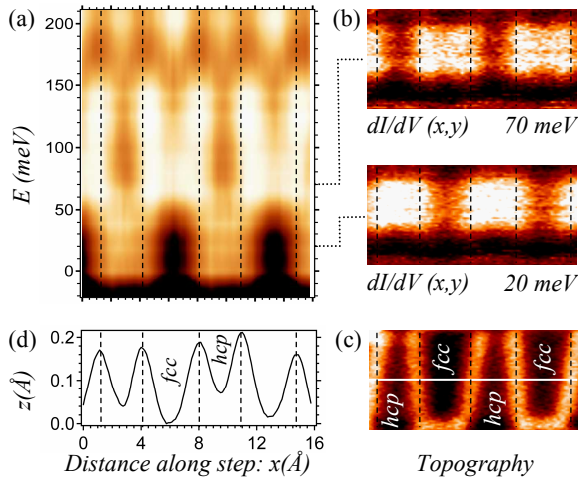


FIG. 3: (color online) (a) dI/dV map obtained by measuring 64 dI/dV spectra along the profile line in (e). (b) dI/dV images at $E=20$ meV and $E=70$ meV illustrating the out-of-phase behavior of the electronic density through the gap. (c) Corresponding topographic image of a terrace (stabilization parameters $I=0.6$ nA, $V_s=-0.65$ V). (d) Constant current line scan in the middle of the terrace along the white line shown in (c).

reflects the reconstruction gap opening as explained on Fig. 2(b). In this image, we present a simulation of the dispersion of the two spin-orbit surface bands in the framework of the nearly free electron model with an effective mass of $m^*=0.265 m$ and a gap value of 40 meV. This picture allows to qualitatively understand the experimental EDC: the dispersionless feature is associated with the two unresolved bands below the gap whereas the two higher energy structures correspond to the two spin-orbit bands above the gap. As discussed above, the Bragg diffraction is found at $k_{\pm} = \pi/L_{sp} \pm \Delta k_{s.o.}/2$ so that the gaps on the two bands appear at the same energy. To be more quantitative, we report in Fig. 2(c) and (d) the four experimental and simulated EDC spectra corresponding to the selected k values. The simulated spectra of Fig. 2(c) have been broadened by a 50 meV-lorentzian and a 0.01 \AA^{-1} -gaussian in order to take into account the excitation lifetime and the angular resolution respectively. The main peak in the 0.0035 \AA^{-1} spectrum corresponds to the two unresolved bands below the gaps whereas the shoulder is due to the weak intensity of the folded band above the gap so that the energy separation between these two spectral features is the gap amplitude. With increasing k , the spectral evolution reflects the balance of spectral weight between bands below and above the gap. At $k=0.075 \text{ \AA}^{-1}$, the two structures are simply associated with the two spin-polarized bands in the second Brillouin zone. The corresponding experimental spectra (Fig. 2(c)) are in good agreement with these simulated ones. They have been adjusted with several

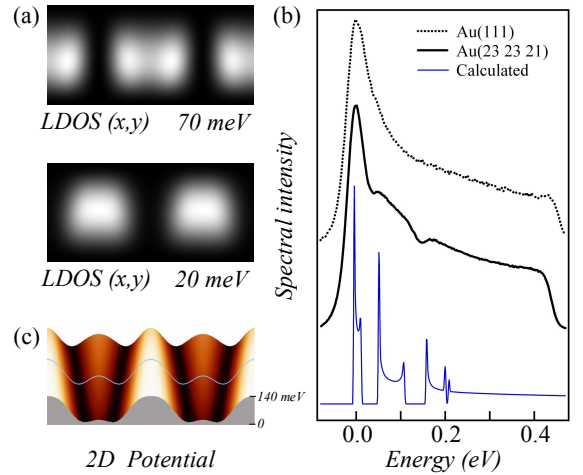


FIG. 4: (color online) (a) Map of the electronic density just below ($E=20$ meV) and above ($E=70$ meV) the first energy gap. (b) Calculated density of states compared with the k_{\parallel} -integrated photoemission spectra for Au(23 23 21) and Au(111). (c) Reconstruction potential used in the calculation.

peaks (dotted lines in Fig. 2(c)) and the energy separation between the low energy structure and the structures appearing with increasing momentum can then be interpreted as the gap amplitude which is estimated to be $\Delta E_{g1} = 40 \pm 5$ meV. The same analysis for the second gap appearing at $E_2 \simeq 145$ meV leads to a gap amplitude of $\Delta E_{g2} = 48 \pm 5$ meV.

In Fig. 3, we present the STS results in an energy range corresponding to the domain where the two gaps appear in photoemission. In the topographic image of a terrace (Fig. 3(c)), the bright stripes correspond to the ridges associated with stacking faults separating fcc and hcp regions of the reconstructed surface. A constant current line scan in the middle of the terrace shows that the hcp region appears slightly higher than the fcc one and both domains are lower than the ridges (Fig. 3(d)). The same behavior has been observed in the herringbone reconstruction of Au(111) and was interpreted as an electronic effect due to a weakly attractive potential in the hcp regions compared to the fcc ones [9, 10]. The differential conductance map of Fig. 3(a) represents the dI/dV spectra for 64 points along the profile line of Fig. 3(c). This image illustrates the variation of the electronic density in energy along the scan line. Close to the energy onset of the surface state, the electronic density is mainly located in the ridges and hcp domains corresponding to low potential regions. A sudden evolution occurs near $E = 45$ meV, the first gap energy. A balance of spectral weight is then observed since above this energy the electronic density is found in the ridges and fcc regions. Therefore, the electronic density exhibits a phase shift of π in its spatial distribution as confirmed in the two dI/dV images of the terrace recorded at $E = 20$ meV

(below) and $E = 70$ meV (above the gap energy). This phase shift behavior is expected in the simple approach of nearly free electron model. However, we would like to point out that some spectral intensity remains in the ridges through this first gap. This behavior was previously reported for the gap induced by a moiré structure of NaCl/Cu(111) [4]. A similar behavior is observed in the energy range corresponding to the second band. Although the electronic density is localized in the ridges and fcc regions just above the 45 meV-gap, a progressive localisation of the density occurs with increasing energy and at $E \simeq 130$ meV, nearly all intensity is localized in the ridges. Around $E = 150$ meV, the local density of states strongly decreases and a sudden change of localisation from the ridges to the hcp and fcc regions is observed. This decrease in the STS signal and the change of the charge density phase reveal the opening of the second gap and corroborate the photoemission results.

These spectroscopic behaviors, i.e. opening of energy gaps by ARPES and spatial modulation of the electronic density by STS, were also observed in Au(788) vicinal surface [18]. They can be describe in the framework of a simple pseudo-potential approach by numerically solving the Schrödinger equation. Indeed, the band structure in the superperiodic Brillouin zone is a direct effect of the reconstruction potential. The main characteristic of the potential can be deduced from our spectroscopic measurements. Firstly, to take into account the electronic confinement in the perpendicular direction, an infinite potential has been chosen for step edges. Secondly, the potential associated with the reconstruction in terraces (fig.1(b)) can be deduced from the magnitude of the gaps determined by photoemission. In the first order perturbation, the gaps are proportional to the magnitudes of the Fourier components of the potential. The observation of only two gaps with similar amplitudes suggests that only the first two Fourier components are important. Moreover, the phase of the electronic density observed in STS shows that these Fourier components are both positive. This leads to an average 1D-potential composed of two components with minima on the ridges (E_{sf}) and maxima on the fcc and hcp domains ($E_{fcc} - E_{sf} = 140$ meV and $E_{hcp} - E_{sf} = 48$ meV, respectively). To take into account the peculiar shape of the reconstruction, we have built a 2D-potential in the superperiodic cell by adapting the respective size of the fcc and hcp domains to keep the potential minima on the ridges. The potential we obtained is presented in the map of Fig. 4(c) for two superperiodic cells. This shape is reminiscent to the one-dimensional potential determined on flat Au(111) from a linear response analysis of the total electron density measured by STM [10]. in our case, the magnitude of the potential we found is larger than the potential deduced on flat Au(111).

This model also allows to calculate the density of states which we have compared with the k_{\parallel} -integrated-

photoemission spectrum (Fig. 4(b)). The photoemission spectrum exhibits the shape characteristic of the one dimensional k-integrated Shockley state [8] but with the presence of two depletions at $E_1=45$ meV and $E_2=145$ meV which confirm the observation of two energy gaps in ARPES data. This experimental spectral density is in satisfactory agreement with the calculated density of states which reproduce the position and amplitude of the gaps [19]. This calculation has been restricted on the fundamental mode of the quantum well (associated with steps) since the excited well states, due to their momentum distribution [11], do not contribute to the photoemission spectra recorded in the plane perpendicular to terraces. Finally, we also present in Fig. 4(a) the calculated electronic density at $E=20$ meV and $E=70$ meV, i.e. on each side of the first gap. These images show the out-of-phase behavior experimentally observed (Fig. 3(b)) and confirm that the Shockley state is localized in the hcp and stacking fault domains below the first gap energy and in the fcc and stacking fault domains above. The agreement between experimental and calculated spectra and dI/dV maps proves that the main physics is captured by this simple model.

In conclusion, we have shown in this paper by ARPES and STS the effects of the reconstruction on the Shockley state of Au(111) vicinal surfaces. In spite of the small amplitude of the reconstruction potential, we succeed to evidence the Bragg diffraction associated with the superperiodicity. This mechanism leads to the formation of several energy gaps with modulation of the electron density. This gap opening was never been observed before probably because the spectral weight essentially remains in the non-reconstructed Brillouin zone with a negligible intensity in the folded bands. Such a reconstructed surface could be a model system to investigate the incompletely understood distribution of photoemission spectral weight in the different Brillouin zones.

-
- [*] corresponding author : malterre@lpm.u-nancy.fr
- [1] J. Anderson and G.P. Lapeyre, Phys. Rev. Lett. **36**, 376 (1996).
 - [2] J.N. Crain, K.N. Altmann, C. Bromberger and F.J. Himpsel, Phys. Rev. B **66**, 205302 (2002).
 - [3] A. Bendounan, F. Forster, J. Ziroff, F. Schmitt and F. Reinert, Phys. Rev. B **72**, 75407 (2005).
 - [4] J. Repp, G. Meyer and K.-H. Rieder, Phys. Rev. Lett. **92**, 36803 (2004).
 - [5] X.Y. Wang, X.J. Shen, R.M. Osgood Jr, R. Haight and F.J. Himpsel, Phys. Rev. B **53**, 15738 (1996).
 - [6] A. Mugarza, A. Mascaraque, V. Pérez-Dieste, V. Repain, S. Rousset, F.J. García de Abajo and J.E. Ortega, Phys. Rev. Lett. **87**, 107601 (2001).
 - [7] M. Hansmann, J.I. Pascual, G. Ceballos, H.-P. Rust and K. Horn, Phys. Rev. B **67**, 121409 (2003).
 - [8] F. Reinert and G. Nicolay, Appl. Phys. A **78**, 817 (2004).

- [9] W. Chen, V. Madhavan, T. Jamneala and M.F. Crommie, *Phys. Rev. Lett.* **80**, 1469 (1998).
- [10] L. Bürgi, H. Brune and K. Kern, *Phys. Rev. Lett.* **89**, 176801 (2002).
- [11] A. Mugarza and J.E. Ortega, *J. Phys.: Condens. Matter* **15**, S3281 (2003).
- [12] J.V. Barth, H. Brune, G. Ertl and R.J. Behm, *Phys. Rev. B* **42**, 9307 (1990).
- [13] S. Rousset, V. Repain, G. Baudot, Y. Garreau and J. Lecoœur, *J. Phys.: Condens. Matter* **15**, S3363 (2003).
- [14] S. LaShell, B. A. McDougall and E. Jensen, *Phys. Rev. Lett.* **77**, 3419 (1996).
- [15] G. Nicolay, F. Reinert, S. Hüfner and P. Blaha, *Phys. Rev. B* **65**, 033407 (2001).
- [16] J. Voit, L. Perfetti, F. Zwick, H. Berger, G. Margaritondo, G. Grüner, H. Höchst and M. Gioni, *Science* **290**, 501 (2000).
- [17] M. Gioni, Ch. R. Ast, D. Pacilé, M. Papagno, H. Berger and L. Perfetti, *New J. Phys.* **7**, 106 (2005).
- [18] C. Didiot et al. to be published.
- [19] A third gap (5 meV wide) is obtained in the calculation and is not large enough to be experimentally observed because of the experimental finite spectral weight due to the lifetime and instrumental broadening.